Journal of Dynamic Systems, Measurement and Control

Technical Briefs

Modeling and Analysis of an Inherently Multi-Rate Sampling Fuel Injected Engine Idle Speed Control Loop

B. K. Powell[1], J. A. Cook[1] and J. W. Grizzle[2,3]

This paper develops a model for the idle speed control of a six cylinder electronically fuel injected, spark ignition engine. The inherently discrete microprocessor based fuel controller is not constrained to operate at the engine's natural sampling rate, resulting in a hybrid (continuous-discrete) multi-rate system. A method for evaluating the stability of the system is developed.

Introduction

The process of an electronically fuel controlled idling engine may be described as a sampled data system consisting of continuous and discrete elements. If the basic engine/power train system is delineated in terms of intrinsic engine events such as breathing, compression and combustion, a discrete model may be developed which incorporates a sampling rate consistent with fundamental engine phenomena. The inherently discrete microprocessor based controller is not constrained to operate at a rate identical to this fundamental frequency. As a result, the overall system may include multiple sampling rates. The idle speed control system on such an engine must maintain the desired engine speed with high accuracy and be robust with respect to disturbances such as automatic transmission neutral-to-drive transition, air conditioner compressor engagement and power steering lock-up.

In this paper, a model will be developed for a six cylinder, electronically fuel injected spark ignition engine. The idle speed control feedback loop will also be developed and a method presented for evaluating the stabiltiy of the closed-loop system.

Model Description

It has been shown that, for some engine control problems, a linear power plant representation may be used as a valid design tool [1, 2, 4–6]. In particular, effective throttle, spark and fuel control strategies have been developed for engine idle speed control in the presence of disturbances. Values of parameters for such models may be obtained from suitable static and dynamic experiments [6] or by the use of dynamic parameter identification techniques [2, 7]. The model employed in this paper follows the general development of [1, 2] augmented to accommodate a six cylinder engine with port fuel injection and arbitrary injection timing. The model contains characterizations of the intake manifold dynamics, the fuel system, the induction-to-power stroke delay, and the rotational dynamics of the power train.

Intake Manifold Dynamics. In a static situation, the mass charge of air and fuel pumped out of the intake manifold by the engine must equal the sum of the air and fuel mass flow rates into the manifold. At idle, the airflow into the manifold is controlled by a limited authority bypass valve. Under constant temperature conditions, a difference in manifold ingress and egress mass flow rates results in a change in manifold pressure. Thus,

$$\dot{P} = K_p(\dot{m}_a + \dot{m}_f - \dot{M}) \tag{1}$$

where

$\dot{P}$ = manifold pressure rate, force/area/time
$\dot{m}_a$ = air mass flow rate, mass/time
$\dot{m}_f$ = fuel mass flow rate, mass/time
$\dot{M}$ = mass flow rate of air plus fuel pumped by the engine, mass/time.

The proportionality constant, K_p is a function of the gas constant, gas molecular weight, specific heat parameters, temperature and manifold volume. The mass flow rate pumped by the engine is a function of cylinder displacement, engine speed, air density and engine volumetric efficiency, which is primarily a function of manifold absolute pressure, P, and engine speed, N. Ultimately then, the mass flow rate, $\dot{M}$, may be represented as a polynomial function of manifold pressure and speed and is often represented as a bilinear function of those variables. The air flow rate into the engine can be represented as a function of manifold pressure and bypass valve position. With this in mind, then, and considering that the air-fuel ratio is much greater than unity (that is, neglecting $\dot{m}_f$), direct linearization of equation (1) yields

$$\tau_p \Delta\dot{P} + \Delta P = \tau_p K_p(K_\theta \Delta\theta - K_N \Delta N) \tag{2}$$

where K_N is a pumping feedback defined by $\partial\dot{M}/\partial N$, K_θ is the air flow rate sensitivity to the air bypass valve position, θ, and the manifold time constant is defined as

$$\tau_p = [K_p(\partial\dot{M}/\partial P - \partial\dot{m}_a/\partial P)]^{-1}, \text{ time.} \tag{3}$$

Throughout this paper, the symbol Δ preceding a variable refers to the perturbation value of the variable about its nominal condition.

Fuel System. The fuel system employed in an electronically controlled fuel injected engine often requires two major operations: air flow sensing and fuel injection timing. The

[1]Scientific Research Laboratory, Ford Motor Co., Dearborn, Mich.
[2]University of Illinois, Coordinated Science Laboratory, Urbana, Ill. 61801
[3]The work of Professor Grizzle was supported in part by the Ford Motor Company and in part by the National Science Foundation under Grant No. ECS-85-05318.

Contributed by the Dynamic Systems and Control Division of The American Society of Mechanical Engineers. Manuscript received by the Dynamic System and Control Division October 1986.

engine type with which this paper is concerned incorporates a method of airflow sensing referred to as speed density. Stated simply, a speed density air sensing system is based upon the calculation of an estimate, defined here as AM, of the mass flow rate quantity $\dot{M}$. Generally, the estimate is calculated as the product of cylinder displacement, engine speed, air density and engine volumetric efficiency at any particular operating point. At such a point, the speed density mass flow rate estimate is given by

$$AM = cPN \tag{4}$$

where

AM = air mass flow rate, mass/time
P = manifold absolute pressure, force/area
N = engine speed, revolutions/time
c = proportionality constant.

Linearizing (4) about the nominal engine idle speed, N_0, and pressure, P_0, yields

$$\Delta AM = c(P_0 \Delta N + N_0 \Delta P). \tag{5}$$

For control to a specified air fuel ratio, A/F, the engine fuel flow rate is proportional to the air flow rate. The actual amount of fuel injected at any one event is proportional to the air flow rate divided by engine speed (which is assumed to be proportional to the air charge).

Induction-to-Power Stroke Delay. A four-stroke spark ignition engine transmits power to the crankshaft via a reciprocating piston and connecting rod. The initial 180° of crankshaft revolution from piston top dead center (TDC) constitute the intake stroke wherein the combustible air and fuel mixture is inducted into the cylinder. Succeeding 180° increments of crankshaft motion make up the compression stroke, which raises the temperature and pressure of the mixture; the power stroke, in which the mixture is ignited resulting in rapid energy release driving the piston downward and imparting power to the crankshaft; and, finally, an exhaust stroke in which the products of combustion are displaced from the cylinder. It is clear that a propagation lag exists between the induction of the fuel-air mixture and the related torque developed at the crankshaft. That is, the combustion torque developed at any instant of time is a function of the mass rates or ratios of mass rates that were sampled one engine induction event earlier. For the linear, six-cylinder engine model, each cylinder is assumed to produce a uniform torque pulse existing over the initial 120° of the power stroke, the magnitude of which is dependent on the sampled engine variables which existed during the previous intake stroke. This results in a continuous, nonoverlapping torque output from the multiple cylinders over the complete 720 deg cycle. In order to be synchronous with the 120 deg torque pulse rate, those variables which contribute to torque (manifold pressure and fuel flow, for example) must be sampled 60 deg before bottom dead center (BDC) of the intake stroke, resulting in an induction to power stroke lag of two sample intervals or 240° (i.e., from 60 deg before BDC of the intake stroke to TDC of the compression stroke). It should be noted that this sample rate is inherent to the six-cylinder engine. Although a faster rate might be employed (resulting in pulsating torque output), the 120 deg rate is the slowest rate consistent with the fundamental breathing and combustion events of the engine.

Hazell and Flower [3] developed a crank angle synchronized relationship for the induction-to-power stroke (IP) lag that is dependent on the number of cylinders and the engine speed. For a given engine speed, N, (rpm), the crankshaft rate is 6N deg/s. For a uniform 120 degree crank angle torque pulse on a six cylinder engine, the time between samples is

$$T = 120\text{deg}/(6\text{N deg/s}) = 20/\text{N s}. \tag{6}$$

Power Train Rotational Dynamics. The rotational motion of the engine crankshaft is given in terms of the engine polar motion of inertia, angular acceleration, and the difference between the net torque generated by the engine and the load torque of the shaft. Crankshaft acceleration is given by

$$J_e \dot{N} = (30/\pi) T_e - (30/\pi) T_L \tag{7}$$

where

J_e = engine inertia, force-distance-time^2/rad
N = engine speed, revolutions/time
T_e = engine net torque output, force-distance
T_L = engine external torque load, force-distance

For a vehicle employing an automatic transmission, the external torque load on the engine consists of the load applied by the torque converter plus external torque disturbances which may arise as a result of auxiliary loads imposed on the engine (engagement of the air conditioner compressor, for example). The torque from the converter is generally specified as the square of the ratio of engine speed to a converter input capacity factor, K_i [1]. The external torque load can then be expressed as

$$T_L = (N/K_i)^2 + T_d. \tag{8}$$

The engine output (or brake) torque has the following functional form:

$$T_e = F(M_d, F_d, \delta, N) \tag{9}$$

where

M_d = mass charge delayed by the IP lag, mass
F_d = fuel delayed by the IP lag, mass
δ = ignition timing, degrees before TDC
N = engine speed, revolutions/time.

The in-cylinder mass charge, M_d, is equal to the mass charge pumped from the engine and delayed by the IP lag. As previously developed, mass charge is a function of manifold pressure, P, and engine speed, N. Because pressure is the dominant variable, engine output torque can be considered to be an implicit function of delayed pressure, P_d. Consequently, linearization of the brake torque relationship yields

$$\Delta T_e = G_P \Delta P_d + G_f \Delta F_d + G_\delta \Delta\delta + F_N \Delta N \tag{10}$$

where G_p is the influence of delayed pressure on torque, G_f, is the influence of delayed fuel on torque, G_δ is the spark advance influence on torque, and F_N is the engine friction, $\partial T_e/\partial N$. The first three terms of equation (10) are sometimes referred to as the combustion torque (or indicated torque), T_c, with perturbation ΔT_c [2, 3]. That is, combustion torque is the engine torque due to the pressure, fuel and spark advance variables and is expressed in linearization form as

$$\Delta T_c = G_p \Delta P_d + G_f \Delta F_d + G_\delta \Delta\delta. \tag{11}$$

Finally, an expression for engine acceleration can be realized by linearization of Newton's equation, (7), with the external load term represented by equation(8) to yield

$$\tau_R \Delta\dot{N} + \Delta N = \tau_R K_R (\Delta T_c - \Delta T_d) \tag{12}$$

where $K_R = 30/(\pi J_e)$ and the rotational time constant is defined as

$$\tau_R = (K_R [2N/K_i^2 + |F_N|])^{-1} \tag{13}$$

Combining equations (2), (11), and (12) with the IP lag on ΔP and ΔF (to provide delayed terms ΔP_d and ΔF_d) yields the linearized, open loop model representation of Fig. 1.

Idle Speed Control

Open loop stability is influenced by the modes associated with the manifold time constant (which is proportional to manifold volume), the IP lag (which is inversely proportional to speed), and rotational dynamics including engine friction and disturbance load damping. Closed loop idle speed stability

can be effected by three control variables: airflow into the engine, ignition timing before TDC and fuel flow. The philosophy imbedded in the idle speed control implementation of this paper is to provide very low gain, pure integral control of the air valve for purposes of steady state accuracy in conjunction with aggressive proportional spark control to enhance speed of response. System stability will be investigated as a function of the control gain on fuel. The fuel injection system which has been modeled consists of one injector located in each of the six runners of the intake manifold close to the cylinder intake port. The amount of fuel to be injected is calculated once per engine revolution based on the speed density airflow. For purpose of economy and simplicity, the injectors are slaved in groups of three and fired alternately at 720 degree crank angle increments delayed 240 degrees from the fuel metering calculation.

It is evident that the inherently discrete injection scheme has a sample rate different from the fundamental engine sampling rate discussed previously. Specifically, the fuel injection rate of once per 360 degress of crankshaft rotation is one third the 120 degree rate required of the six cyliner engine. For purposes of discretization, the engine model thus far developed may be sampled at its fundamental rate with the first sample occuring at TDC of the intake stroke and the fuel injection samples occuring synchronously at one third the fundamental rate. A block diagram of the linearized, hybrid, multi-rate system incorporating the speed density fuel system as well as spark and airflow feedback is illustrated in Fig. 2.

Idle Stability Analysis

The presence of multiple sampling rates in the model which has been presented makes the stability analysis of the system a nonstandard problem. In this section, an analytical technique which reduces the stability question to that of an associated single-rate system is presented. Significant extensions of the basic idea will appear in [10].

A Simple Multi-Rate System. Consider the control system illustrated in Fig. 3 where the subsystem $G(z)$ in the forward path operates at a sampling period T and the subsystem $H(\hat{z})$ in the feedback path operates at a sampling period $\hat{T}$; z and $\hat{z}$ are the z-transform variables for the respective sampling periods; the samplers are included in order to emphasize that the discrete-time subsytems $G(z)$ and $H(\hat{z})$ operate at different rates. It is supposed that $\hat{T} = iT$, where i is a positive integer, and that u and d are constant over intervals of length T and $\hat{T}$, respectively; d represents a disturbance or measurement error. Such a system will be said to be bounded-input bounded-

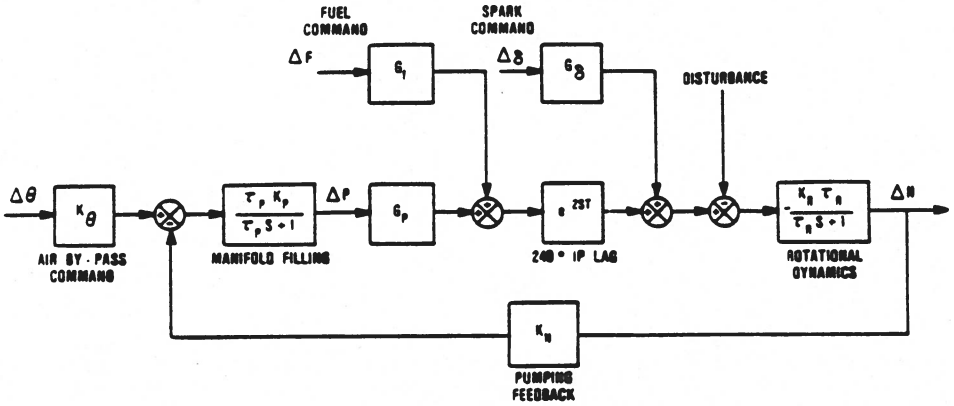

Fig. 1 Linearized open-loop six cylinder engine dynamic model.

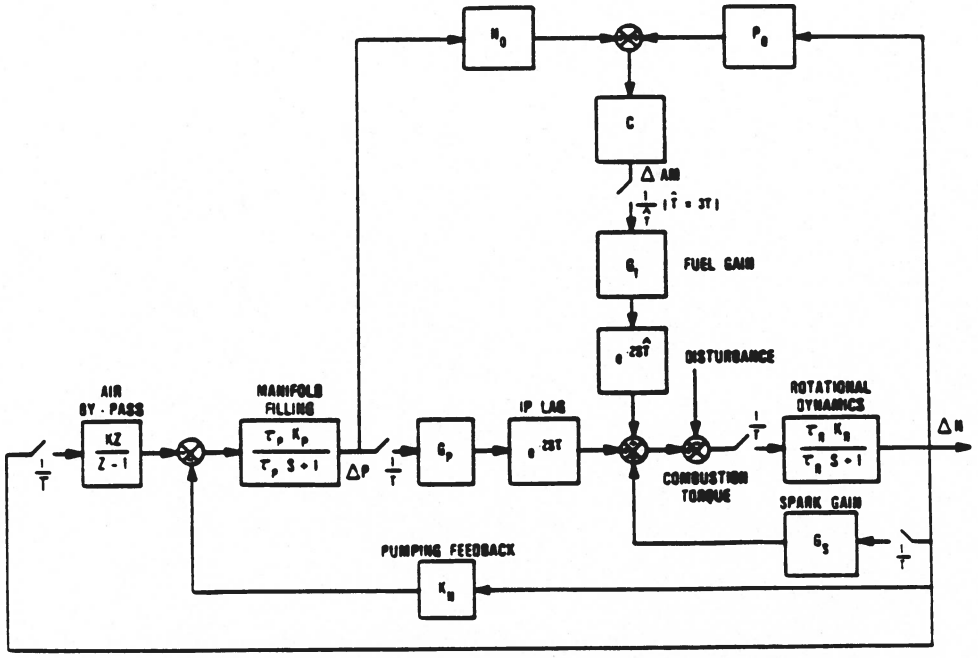

Fig. 2 Linearized closed-loop six cylinder engine dynamic model.

output (BIBO) stable if a bounded control, u, and disturbance, d, (inputs) always result in a bounded measurement, y, and error, e, (outputs).

The important question is how the stability of the overall system can be determined from $G(z)$, $H(\hat{z})$ and i. Toward this end, an associated single-rate system is now constructed.

Let

$$x_{k+1} = Ax_k + Be_k.$$

$$y_k = Cx_k \tag{14}$$

be a state space realization of $G(z)$; i. e.,

$$G(z) = C(zI - A)^{-1}B.$$

Suppose now that u is constant over intervals of length $\hat{T} = iT$ so that e is then constant over intervals of this length. Iterating (14) i times yields

$$x_{(j+1)i} = A^i x_{ji} + \left(\sum_{\alpha=0}^{i-1} A^\alpha B\right) e_{ji} \tag{15}$$

$$y_{ji} = Cx_{ji}$$

Defining $\hat{x}_j = x_{ji}$, $\hat{e}_j = e_{ji}$, $\hat{y}_j = y_{ji}$, $\hat{A} = A^i$, $\hat{B} = \left(\sum_{\alpha=0}^{i-1} A^\alpha B\right)$

and $\hat{C} = C$, one obtains the system

$$\hat{x}_{j+1} = \hat{A}\hat{x}_j + \hat{B}\hat{e}_j$$

$$\hat{y}_j = \hat{C}\hat{x}_j \tag{16}$$

which exactly reproduces the ith output value of (14) when u (and hence e) is constant over intervals of length iT. The role of this derived system in assessing the stability of the original multi-rate control system of Fig. 3, where u is only assumed constant over intervals of length T, is now established.

Main Stability Result. Let $\hat{G}(\hat{z}) := \hat{C}(\hat{z}I - \hat{A})^{-1}\hat{B}$ be the transfer function of (16). Then, if $G(z)$ and $\hat{G}(z)$ have the same number of unstable poles, the multi-rate feedback system of Fig. 3 is BIBO stable if and only if the single-rate feedback system of Fig. 4 is BIBO stable.

A proof of this result is outlined in the Appendix. Some additional remarks are useful:

(*a*) The system of Fig. 4 is BIBO stable if and only if

$$\begin{bmatrix} (I + H\hat{G})^{-1} & -(I + H\hat{G})^{-1}H \\ (I + \hat{G}H)^{-1}\hat{G} & -(I + \hat{G}H)\hat{G}H \end{bmatrix} \tag{17}$$

has all its poles in the open unit circle [8].

(*b*) If all the poles of H are in the open unit circle, then (17) has all its poles in the open unit circle if and only if the poles of $(I + \hat{G}H)^{-1}\hat{G}$ are within the open unit circle [8]; i.e., the sytem is stable in the usual sense [8, 9].

(*c*) The hypothesis that $G(z)$ and $\hat{G}(\hat{z})$ have the same number of unstable poles simply assures that iterating (14) has not caused an unstable mode of $G(z)$ to become hidden; generically, it is always satisfied.

(*b*) In the case that G and H are SISO subsytems, then Remark (*b*) reduces the stability analysis of the multi-rate system to that of a standard SISO root locus analysis. This property is not enjoyed by the results of [11], for example.

Idle Speed Loop Stability Analysis. The stability result developed above can now be applied to the idle speed control system illustrated in Fig. 2. Substituting numerical parameter values based upon six-cylinder engine data, and using standard techniques to discretize the forward and feedback paths results in the system illustrated in Fig. 5, with the control gain of interest, K_f. Mathematically,

$$G(z) = \frac{0.188z^4 - 0.346z^3 + 0.158z^2}{z^5 - 2.73z^4 + 2.49z^3 - 0.725z^2 - 0.0016z - 0.027} \tag{18}$$

and

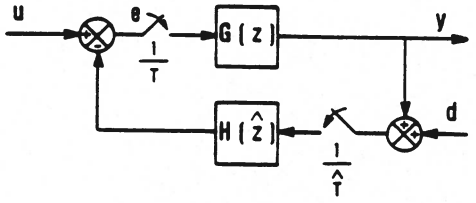

Fig. 3 Multirate system

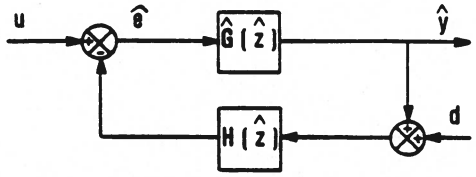

Fig. 4 Associated single-rate system

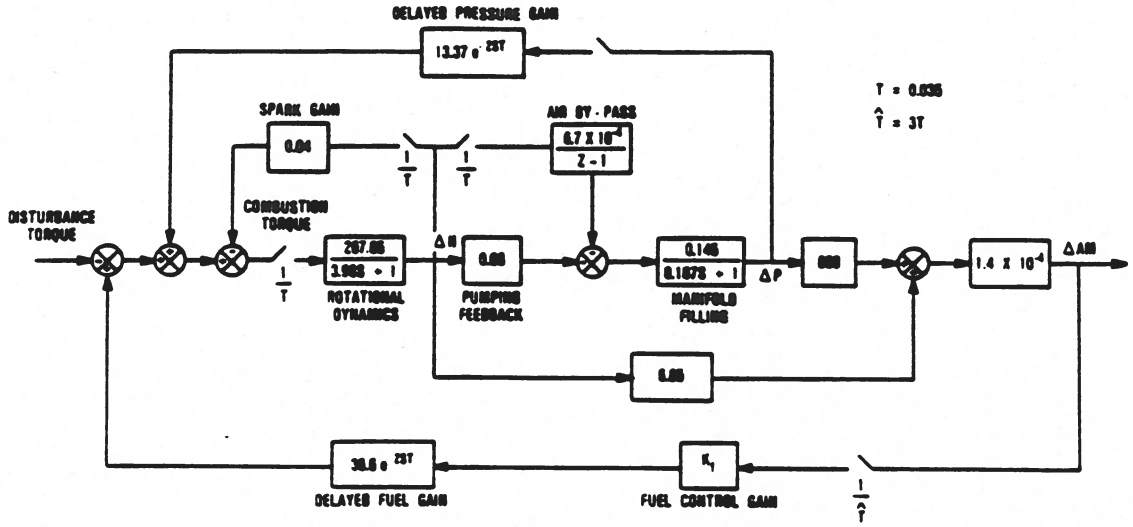

Fig. 5 Multirate idle speed control system

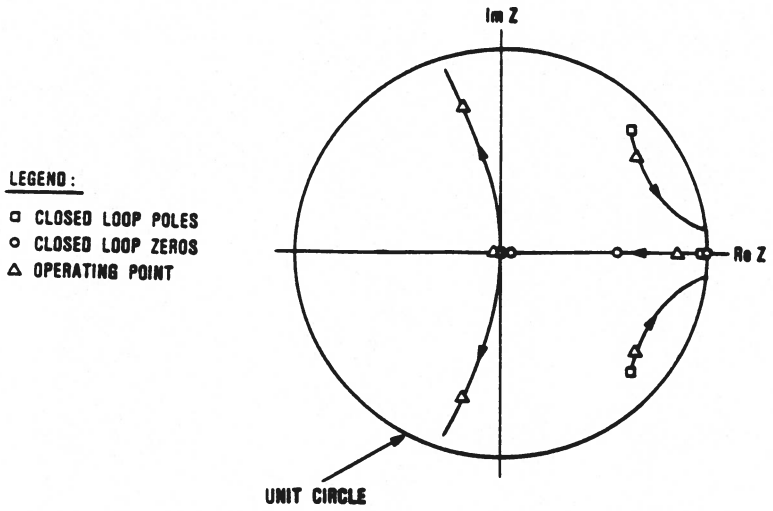

Fig. 6 Root locus of the idle speed control system

$$H(\hat{z}) = \frac{K_f\,(36.6)}{\hat{z}}. \tag{19}$$

Applying the method outlined above yields

$$\hat{G}(\hat{z}) = \frac{0.512\hat{z}^4 - 0.830\hat{z}^3 + 0.337\hat{z}^2 - 0.018\hat{z} + 1.2\times 10^{-4}}{\hat{z}^5 - 2.229\hat{z}^4 + 1.969\hat{z}^3 - 0.736\hat{z}^2 + 0.006\hat{z} - 2\times 10^{-5}}. \tag{20}$$

Since $G(z)$ and $\hat{G}(\hat{z})$ have no unstable poles, the main result presented above is applicable. Moreover, since all the poles of $H(\hat{z})$ are strictly within the unit circle, remark (*b*) is applicable and hence the stability of the overall system is equivalent to the poles of

$$\frac{\hat{G}(\hat{z})}{1 - K_f\hat{G}(\hat{z})H(\hat{z})}$$

being inside the unit circle. Note that for the system of Fig. 5, the feedback is positive. A root locus analysis illustrated in Fig.6 shows the system to be stable for a range of gains, K_f.

Summary

A multi-sampling rate model of a six cylinder engine has been presented. The fast sampling rate associated with the basic engine was determined by the fundamental breathing and combustion characteristics of the plant; the slow sampling rate of the fuel system was determined by the fuel injection timing characteristics. A method was presented to transform the multi-rate system to a single-rate system amenable to conventional stability analysis.

Acknowledgments

The authors wish to thank the reviewers of their careful comments and Kevin Beuscher for valuable discussions on multi-rate digital systems. The third author thanks the Ford Motor Co. for the opportunity to work in the pleasant and stimulating atmosphere of the Gas Turbine Laboratory and the Scientific Research Laboratory.

References

1 Powell, B. K., and Powers, W. F., "Linear Quadratic Control Design for Nonlinear IC Engine Systems," *Proc. Intl. Society of Automotive Technology and Automation*, Stockholm, Sweden, Oct. 1981.

2 Morris, R. L. and Powell, B. K., "Modern Control Applications in Idle Speed Control," *Proc. of American Control Conf.*, Vol. 1, June 1983, pp. 79-85.

3 Hazell, P. A., and Flower, J. O., "Sampled Data Theory Applied to the Modeling and Control Analysis of Compression Ignition Engines-Part I," *Int. J. of Control*, Vol. 13, No. 3, 1971, pp. 549-562.

4 Dobner, D. J., "Dynamic Engine Models for Control Development-Part I: Nonlinear and Linear Model Formulation," *Application of Control Theory in the Automotive Industry*, Interscience Publication, Geneva, Switzerland, 1983.

5 Dobner, D. J., and Fruechte, R. D., "An Engine Model for Dynamic Engine Control Development," *Proc. American Control Conf.*, Vol 1, June 1983, pp. 73-78.

6 Coats, F. E. and Fruechte, R. D., "Dynamic Engine Models for Control Developement-Part II: Application to Idle Speed Control," *Application of Control Theory in the Automotive Industry*, Interscience Publication, Geneva, Switzerland, 1983.

7 Morris, R. L., Borcherts, R. H., Worlick, M. V., and Hopkins, H. G., "Spark Ignition Engine Model Building—An Identification Approach to Throttle-Torque Response," *Int. J. Vehicle Design*, Vol. 3, No. 1, 1982.

8 Vidyasagar, M., *Control System Synthesis: A Factorization Approach*, MIT Press, Cambridge, MA, 1985.

9 Chen, C. T., *Linear System Theory and Design*, Holt, Rinehart and Winston, New York, 1984.

10 Beuscher, K., Masters Thesis, Department of Electrical and Computer Engineering, University of Illinois at Urbana-Champaign, December 1987.

11 Araki, M, and Yamamoto, K., "Multivariable Multirate Sampled-Data Systems: State-Space Description, Transfer Characteristics, and Nyquist Criterion," *IEEE Trans, Automat. Contr.*, Vol. AC-31, No. 2, Feb. 1986, pp. 145-154.

APPENDIX

Suppose the system illustrated in Fig. 4 is not BIBO stable. Then there exists a bounded control, u, and a bounded disturbance, d, such that $\lim_j \sup \|\hat{y}_j\| = \infty$ and/or $\lim_j \sup \|\hat{e}_j\| = \infty$. For definiteness assume the former. Then $\lim_{ji} \sup \|y_{ji}\| = \infty$, from which one deduces that $\lim_k \sup \|y_k\| = \infty$. Hence, the system illustrated in Fig. 3 is not BIBO stable. The other case is similar.

To show the other direction, suppose that the system of Fig. 4 is BIBO stable. Let

$$\begin{aligned} w_{j+1} &= Lw_j + Mv_j \\ N_j &= Nw_j \end{aligned} \tag{A.1}$$

be a state space realization of $H(\hat{z})$. Without loss of generality, one can suppose that (14) and (A.1) are stablizable and detectable [8, 9]. Since G and $\hat{G}$ have the same number of unstable poles, (16) is then also stabilizable and detectable.

A state space representation of Fig. 4 is

$$\begin{bmatrix} \hat{x}_{j+1} \\ w_{j+1} \end{bmatrix} = \left[\begin{array}{c|c} A^i & -\sum_{\alpha=0}^{i-1} A^\alpha BN \\ \hline MC & L \end{array}\right] \begin{bmatrix} \hat{x}_j \\ w_j \end{bmatrix} + \left[\begin{array}{c|c} \sum_{\alpha=0}^{i-1} A^\alpha B & 0 \\ \hline 0 & M \end{array}\right] \begin{bmatrix} \hat{u}_j \\ d_j \end{bmatrix}$$

$$\begin{bmatrix} \hat{y}_j \\ \hat{e}_j \end{bmatrix} = \begin{bmatrix} C & 0 \\ 0 & -N \end{bmatrix} \begin{bmatrix} \hat{x}_j \\ w_j \end{bmatrix} + \begin{bmatrix} 0 \\ I \end{bmatrix} \hat{u}_j \tag{A.2}$$

which by hypothesis is BIBO stable; combined with the stabilizabiltiy and detectability of the state space realizations of $\hat{G}$ and H, it follows that (A.2) is internally stable [8] (i.e., its eigenvalues are all in the open unit circle). This yields that the system

$$\begin{bmatrix} \hat{x}_{j+1} \\ w_{j+1} \end{bmatrix} = \left[\begin{array}{c|c} A^i & -\sum_{\alpha=0}^{i-1} A^\alpha BN \\ \hline MC & L \end{array}\right] \begin{bmatrix} \hat{x}_j \\ w_j \end{bmatrix} + \begin{bmatrix} \sum_{\alpha=0}^{i-1} A^\alpha Bu_{ij+\alpha} \\ Md_j \end{bmatrix}$$

$$\begin{bmatrix} \hat{y}_j \\ \hat{e}_j \end{bmatrix} = \begin{bmatrix} C & 0 \\ 0 & -N \end{bmatrix} \begin{bmatrix} \hat{x}_j \\ w_j \end{bmatrix} + \begin{bmatrix} 0 \\ I \end{bmatrix} \hat{u}_j \tag{A.3}$$

which describes the evolution of every ith value of the outputs of Fig. 3, is internally stable. Thus, the boundedness of the inputs u_j and d_j entails that of all the internal and external signals $\hat{x}_j$, w_j, $\hat{y}_j$, and $\hat{e}_j$. This establishes immediately the boundedness of e_k, for all k, since $e_{ij+\alpha} = u_{ij+\alpha} - Nw_j$, for $\alpha = 0, \ldots, i-1$. The boundedness of y_k, for all k, follows from

$$\|y_{ij+\alpha}\| \leq \|CA^{\alpha-1}\| \, \|\hat{x}_j\| + \| \sum_{m=0}^{\alpha=1} CA^m B \| \, \|e_{ji+m}\|.$$

This completes the proof.